

A Spiral Cavity Backed 4×4 MIMO SIW Antenna at Ku Band for Radio Telescopes

Suryansh Saxena*, Nidhi Tewari, and Shweta Srivastava

Department of Electronics and Communication Engineering, Jaypee Institute of Information Technology, Noida, India

ABSTRACT: A compact spiral cavity backed substrate integrated waveguide (SIW) multiple input multiple output (MIMO) antenna is presented in this paper. The edge-shaped spiral on top of the SIW cavity acts as a dipole antenna. The dual spiral arms are excited from their symmetrical connecting center. The single antenna element in MIMO is rotated such that unit cells are orthogonal to each other, forming a compact 2×2 and 4×4 MIMO SIW antenna. The proposed design shows a wide bandwidth of 930 MHz (13.74 GHz to 14.67 GHz) and 67.68% impedance bandwidth. The overall size of proposed MIMO SIW antenna is $0.9\lambda_o \times 0.9\lambda_o \times 0.024\lambda_o$, where λ_o is the operating wavelength. A return loss of 18.4 dB at 14.17 GHz is achieved. The series of metal pins (in plus shape) at the center of 4×4 MIMO improves the isolation to 19.6 dB at resonant frequency. A pattern diversity in broadside direction is achieved by the top spiral arms and its complementary spiral arms at the bottom. The beamwidth of the proposed antenna is 90° varying from -45° deg to $+45^\circ$ deg, useful for reliable signal transmission and reception. Thus, the proposed antenna is a symmetrical compact design working at Ku band suitable for radio telescope application.

1. INTRODUCTION

Radio telescopes are powerful instruments used to observe the universe in radio frequencies [1, 2]. They play a crucial role in astronomy, astrophysics, and cosmology, helping scientists understand celestial phenomena such as pulsars, quasars, and cosmic microwave background radiation. Multiple input multiple output (MIMO) antenna technology is now integrated into radio and telescopic applications to improve signal reliability, system overall performance, and high throughput. In MIMO technology, using multiple antennas at transmitter and receiver improves signal quality and reception. Some of the advantages are: First is the ability to detect weaker signals from distant celestial objects, increasing the sensitivity of radio telescopes. Second is signals from multiple antennas, and MIMO systems can achieve higher spatial resolution improving the clarity and detail of the images produced by radio telescopes and allowing for more precise observations and measurements. This allows astronomers to observe faint cosmic phenomena that would otherwise go undetected. Third is that MIMO systems can exploit diversity gain to enhance signal quality and reduce the impact of radio frequency interference (RFI), leading to clearer and more accurate observations.

By enhancing signal reception, increasing data throughput, mitigating interference, and providing scalability, MIMO technology enables radio telescopes to achieve unprecedented levels of sensitivity, resolution, and accuracy. The integration of MIMO antennas into radio telescopic applications represents a significant advancement in the field of radio astronomy. This technological leap opens new frontiers for exploring the universe, unraveling its mysteries, and advancing our understand-

ing of the cosmos. Researchers have explored various MIMO antenna design approaches using microstrip technology [3]. Recently MIMO antennas have been designed on flexible and transparent substrates too given in [4, 5]. However, these antennas suffer from low gain and fabrication complexity specifically at higher frequencies. At higher frequency substrate integrated waveguide (SIW) technology provides the opportunity for low cost, low insertion loss, planar integration, and hence high quality factor [6]. Cavity backed SIW has played a key role in array, multiplexing and duplexing antennas [7–13]. The advantage of cavity backed SIW antennas is the size compactness and high gain with minimum losses (due to confined structure). MIMO technology is integrated with cavity backed SIW technology to achieve compact structures, high isolation, and high gain system. In 2023, Tewari et al. proposed a self-isolation based cavity backed SIW MIMO antenna working at Ka band with high gain [14, 15].

An Archimedean spiral SIW antenna, in particular, has garnered attention for its design and performance benefits. Spiral antennas are known for wide bandwidth, circular polarization, and frequency independent antennas suitable for various applications, including wireless communications, radar systems, and satellite communications [16]. Archimedean spiral SIW antenna is a specific implementation that leverages the SIW approach to enhance the traditional spiral antenna's performance. Key characteristics include: compact size, circular polarization, and ease of fabrication. Researchers have explored different configurations to achieve circular polarization in SIW antennas [17, 18]. In literature, cavity backed SIW dual spiral arm antenna is an area that needs attention showing more opportunities in this field. Compared to circular spiral antenna designs,

* Corresponding author: Suryansh Saxena (s.saxena@se24.qmul.ac.uk).

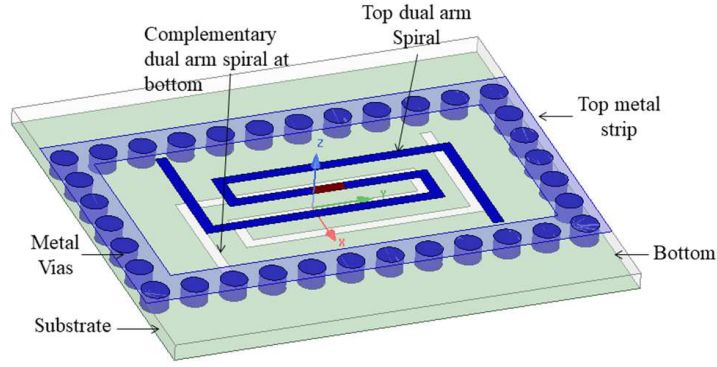


FIGURE 1. Unit cell of dual arm spiral cavity backed SIW antenna.

rectangular spiral antenna is more suitable in terms of compactness and gain. Similar concept is used in the paper to design a compact MIMO antenna.

In this paper, we present an edge shaped spiral SIW MIMO antenna with its complementary structure configuration. The paper is categorized in following sections. Section 1 presents the basic designing of complementary cavity backed spiral SIW antenna (CCBSSA). Section 2 covers the result and discussion on parametric analysis of antenna, followed by design and results of CCBSSA MIMO with the help of graphs and plots. Section 3 covers the diversity performance analysis of MIMO antenna, and Section 4 covers the conclusion and learning outcome of proposed antenna design.

2. ANTENNA DESIGN METHODOLOGY

SIW rectangular cavity is designed to operate in desired operating frequency which lies in Ku band region with minimum leakage losses. The substrate is Rogers RT/Duroid 5880 with a relative permittivity of 2.2 and a loss tangent of 0.0009. The cavity backed spiral SIW antenna is shown in Fig. 1. The dimensions of the cavity backed SIW are calculated based on the resonant frequency of 14 GHz [7] from Equations (1)–(3).

$$f_r = \frac{2c}{\sqrt{\epsilon_r}} \sqrt{\left(\frac{m}{W_{eff}}\right)^2 + \left(\frac{q}{L_{eff}}\right)} \quad (1)$$

where

$$L_{eff} = L_{siw} - \frac{d^2}{0.95p} \quad (2)$$

$$W_{eff} = W_{siw} - \frac{d^2}{0.95p} \quad (3)$$

Here, c is the speed of light (m/sec); f_r is the resonant frequency in Hz; m and q are the modes of cavity resonator; W_{eff} is the width of rectangular cavity; L_{eff} is the length of the cavity resonator; L_{siw} is the length of SIW cavity; W_{siw} is the width of SIW cavity; d is the diameter of the metal vias; and p is the pitch of vias. The curve equation of a dual Archimedean spiral single arm r_1 of the antenna is calculated from the following Equation (4) given in [20]:

$$r_1 = r_{in} + a\phi \quad (4)$$

Here, r_{in} is the inner radius of spiral arm, a the increased rate of spiral (constant), and ϕ the spoke angle. The two arms of the Archimedean spiral antenna are 180° out of phase to each other. The equation for the second arm r_2 becomes (5):

$$r_2 = r_{in} + a(\phi - \pi) \quad (5)$$

The proportional constant ‘ a ’ is also known as growing rate of spiral arms. It is calculated from following Equation (6):

$$a = \frac{(L_{in} + W_s)}{\pi} \quad (6)$$

Here, L_2 is the space between the arms, and W_{gap} is the width of each arm. The space between arms, i.e., L_{in} , is calculated from following Equation (7):

$$L_2 = \frac{(r_{out} - r_{in})}{2N - W_{siw}} \quad (7)$$

Here, the number of turns of the spiral is denoted by N , and r_2 is the distance from the center to the outer arm of the spiral. The inner radius r_{in} (approx. equal to $\lambda/4$) is proportional to lower frequency point, and r_{out} (is the total length of arm from center or circumference of the spiral) is proportional to higher frequency point for an operating frequency range.

The CCBSSA design is structured in three layers: top, substrate, and bottom layers shown in Fig. 1. The top layer consists of the dual spiral arms of metal strips in rectangular shape (acting as dipole), along with a field boundary of copper strip covering the row of metal vias, to ensure the center feeding of dual arm spiral antenna and avoid spurious surface radiation of antenna. The middle layer consists of a substrate with a SIW cavity formed by a row of metal vias. The proper selection of diameter and pitch of vias minimizes the leakage loss and band-gap effect phenomenon in SIW. Certain guidelines are mentioned in [19] to calculate the value of diameter and pitch of vias in SIW. The bottom layer consists of a complementary structure of spiral arms, consisting of the same dimensions but with a mirror image just below the top spiral, such that the feeding port lies at the center of top and bottom spirals shown in Fig. 2 with design parameters.

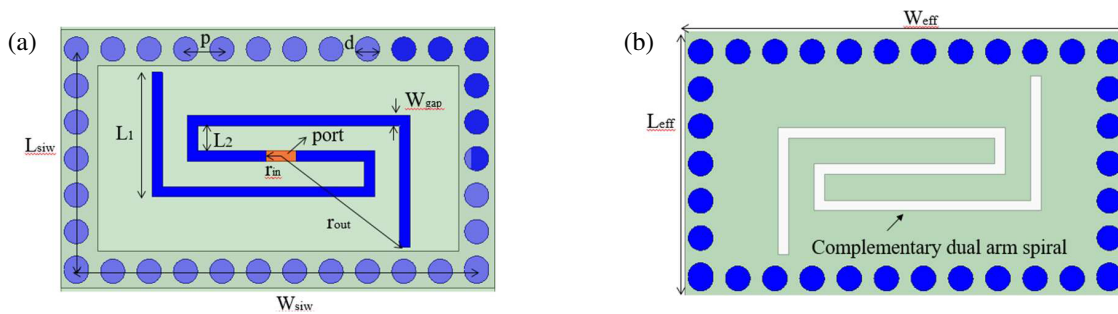


FIGURE 2. Unit cell of arm spiral cavity backed SIW antenna with design parameters and top/bottom view. $L_1 = 3.76$ mm, $L_2 = 0.83$ mm, $r_{in} = 0.5$ mm, $r_{out} = 4.83$ mm, $W_{gap} = 0.34$ mm, $W_{siw} = 7.25$ mm, $L_{siw} = 13.2$ mm, $W = 7.25$ mm, $L = 13.2$ mm, $p = 1.2$ mm, $d = 0.8$ mm and width of metal strip above vias = 3 mm. (a) Top view and (b) Bottom view.

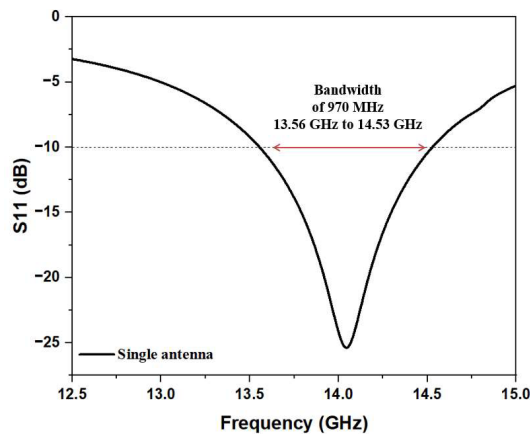


FIGURE 3. S_{11} response of unit cell CCBSSA resonating at 14.17 GHz.

3. RESULT ANALYSIS AND DISCUSSION

3.1. Unit Cell CCBSSA

The region where the spiral's circumference equals one wavelength is where the Archimedean spiral antenna radiates waves. The unit cell consists of dual spiral arms connected through a coaxial port at the center such that the arms are 180° to each other (can be seen in Fig. 2). A complementary structure of spiral is etched at the bottom ground plane which improves the impedance matching. The unit cell of complementary cavity backed spiral-arms SIW antenna (CCBSSA) radiates at 14.17 GHz with a return loss of 25 dB ($S_{11} < |-10|$ dB impedance bandwidth) as shown in Fig. 3. The port excited at the center of dual arm spiral with polarities positive (+) and negative (-) triggers the current to flow in each arm. The number of turns in spiral arm influences the operating bandwidth of the antenna, but increase in exponential rate of turns is limited to the decaying of current as well. The number of optimized turns is limited to three after which current extends to zero, and antenna does not radiate.

The field distribution plot is shown in Fig. 3, where current flows from center coaxial feed towards each arm of spiral along the length at 14.17 GHz. Also, it can be seen that fields are confined in the cavity, by the electric field boundary wall of a metal strip of width 3 mm. The metal strip is placed above the metal vias from all four sides to avoid any leakage of power and efficient radiation of spiral arms, as seen in Fig. 4. The

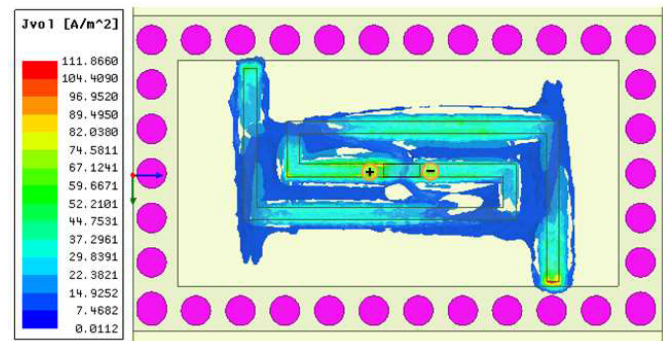


FIGURE 4. Field distribution of CCBSSA unit cell at 14.17 GHz.

top spiral arms radiate in broadside direction (i.e., perpendicular to antenna plane or maximum radiation at 0° in E -plane). Similarly, its complementary spiral arms at bottom plane radiate at 180° in E -plane. Thus, an eight shape radiation pattern is achieved in CCBSSA design. It can be verified from 2D plot radiation pattern of unit cell CCBSSA for co- and x-pol in E - and H -planes, shown in Fig. 5. Due to spiral arms at top and bottom of the SIW cavity, CCBSSA radiates in both the directions which helps to achieve pattern diversity.

3.2. Parametric Analysis

Upon parametric analysis of the proposed design by changing the length of the arm and providing it with variations ranging from 2 mm to 2.4 mm, a pattern in the S_{11} is observed as shown in Fig. 6(a). It can be clearly inferred that 2.25 mm is considered as the optimum length of the spiral at which the bandwidth and return loss are maximum. As the length increases, there is a slight change in the return loss.

Similarly on changing the width of the spiral arm as shown in Fig. 6(b), the frequency is shifted towards a higher side, which indicates that by decreasing the width of the spiral arm, the frequency can be shifted towards higher side. The optimal value of 0.34 mm is the width of the spiral arm selected based on required operating frequency.

3.3. A Spiral Cavity Backed MIMO SIW Antenna

The spiral arms of each antenna are structured in a compact manner to design MIMO SIW antennas. Here four unit cells

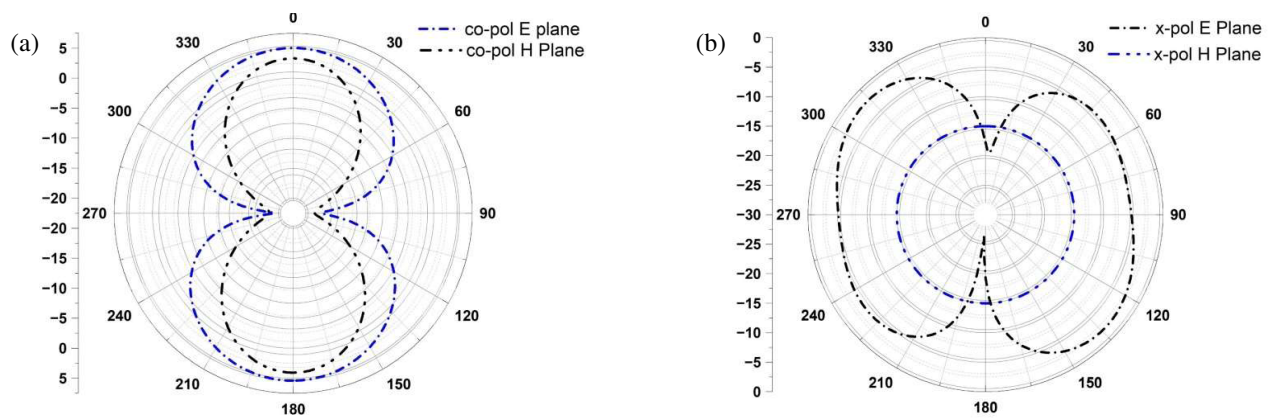


FIGURE 5. A 2D-plot radiation pattern of unit cell CBSSA in (a) *E*- and *H*-coplane and (b) *E*- and *H*- x-pol plane at 14.17 GHz.

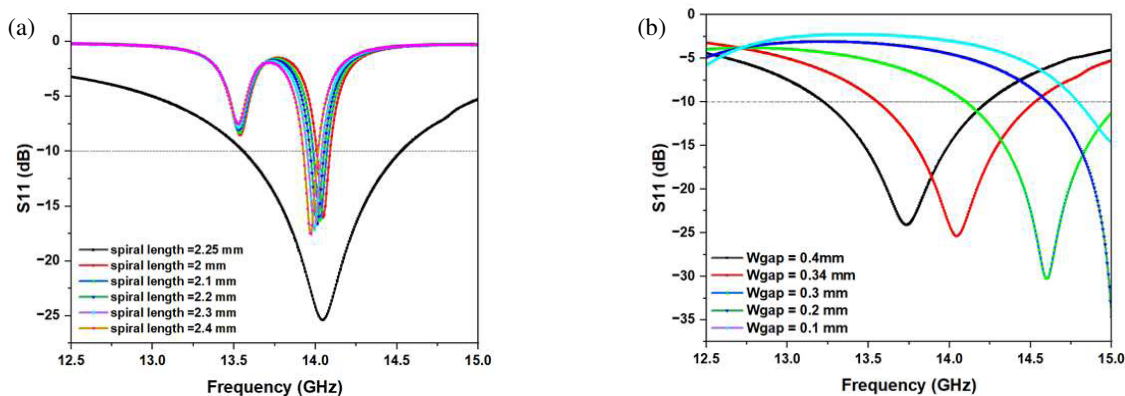


FIGURE 6. Parametric analysis of dual spiral arms (a) length and (b) width (W_{gap}).

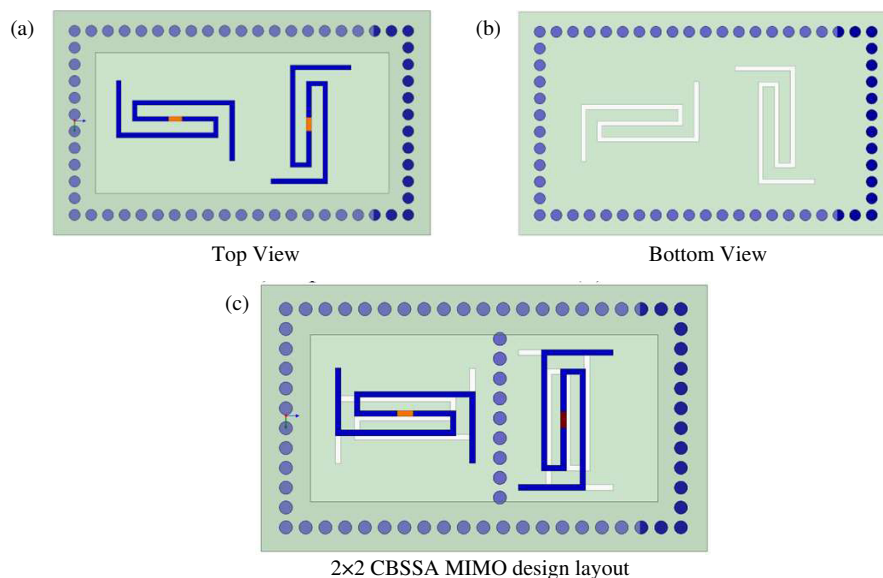


FIGURE 7. A 2×2 CBSSA MIMO antenna design is shown in figure above (a) and (b) without and (c) with metal vias wall. The ports are shown in orange color for each antenna.

of CCBSSA are rotated and placed orthogonal to each other to minimize the coupling of radiation pattern, surface current coupling and increase isolation between any two antennas as shown in Fig. 7 (2×2 MIMO CBSSA) and Fig. 9 (4×4 MIMO CCB-

SSA), with top and bottom views for each MIMO antenna. The 2×2 MIMO CCBSSA is measured and simulated resonating at 14.2 GHz with S_{11} of -21.8 dB and S_{21} of -33 dB shown in

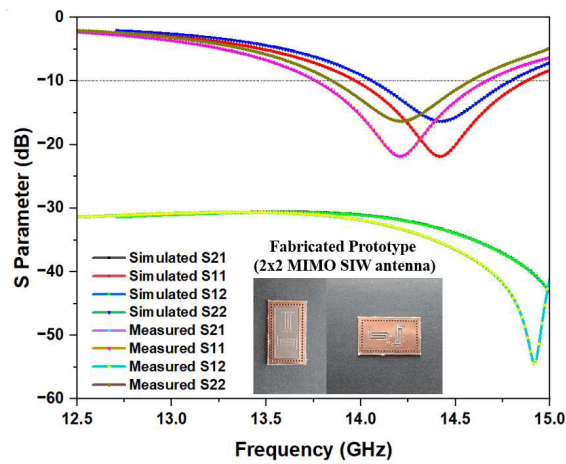


FIGURE 8. Simulated and measured 2×2 CBSSA MIMO antenna S -parameter results are shown with fabricated prototype resonating at 14.21 GHz and bandwidth of 900 MHz.

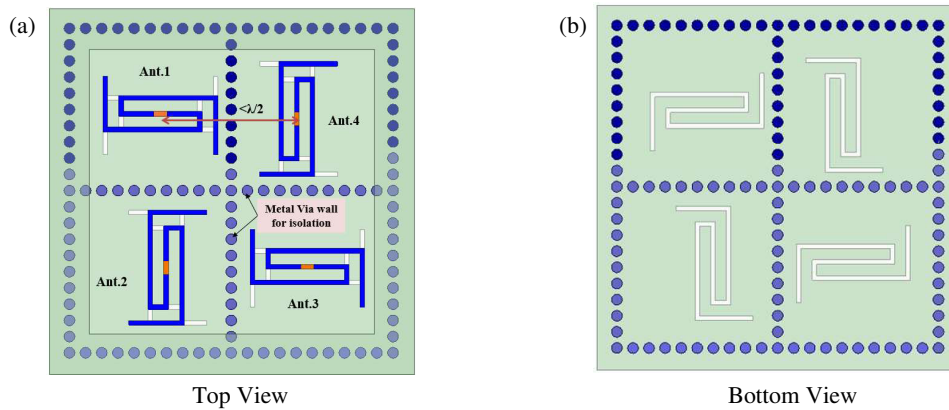


FIGURE 9. Proposed CBSSA 4×4 MIMO antenna design with top view and bottom view is shown in (a) and (b).

TABLE 1. Comparison among simulated Archimedean spiral unit cell, 2×2 and 4×4 MIMO SIW antennas.

Antenna Design	f_r (GHz)	S_{11} (dB)	S_{21} (dB)	Gain (dBi)
Unit Cell	14.17	-25	-	5.1
2×2 MIMO SIW without Isolation	14.21	-20.5	-28	5.1
2×2 MIMO SIW with Isolation	14.21	-21.8	-33	5.2
4×4 MIMO SIW without Isolation	14.2	-20.46	-20.45	5.6
4×4 MIMO SIW with Isolation	14.17	-18.4	-19.6	5.4

Fig. 8, with fabrication prototype. The measured S parameter results are in a good match with the simulated ones.

To design a compact MIMO antenna, mutual coupling or isolation between antennas degrades. The distance required to avoid mutual coupling between any two antennas should be approximately $\lambda/2$. In the proposed 4×4 MIMO CCBSSA, the distance from port1 to port2, port2 to port3, and port3 to port4 is 10.3 mm which is less than $\lambda/2$ as shown in Fig. 9. Thus, to avoid any interference and radiation leakage between the elements, vias in the form of a '+' is placed. The placement of vias in the given design provides additional isolation to each element from the adjacent one. This improves isolation shifting resonant frequency to 14.17 GHz.

Table 1 shows the comparison and improvement of isolation and gain in unit cell, 2×2 and 4×4 CCBSSA MIMO antennas. The measured and simulated S parameter graphs display a good matching of -18.4 dB as well as a good isolation of -19.6 dB at 14.17 GHz seen in Fig. 10 (with fabricated prototype). The measured resonating frequency is found to be approximately 14.25 GHz. The shift in the resonating frequency between measurement and simulation is due to coaxial port at center feeding of dual spiral arms and fabrication error (due to soldering and phase cable losses). Further, the current distribution for the 4×4 CCBSSA MIMO antennas is shown in Fig. 11. It can be clearly seen in Fig. 11 that when antenna element 1 is excited, all the current and radiation are confined only to the

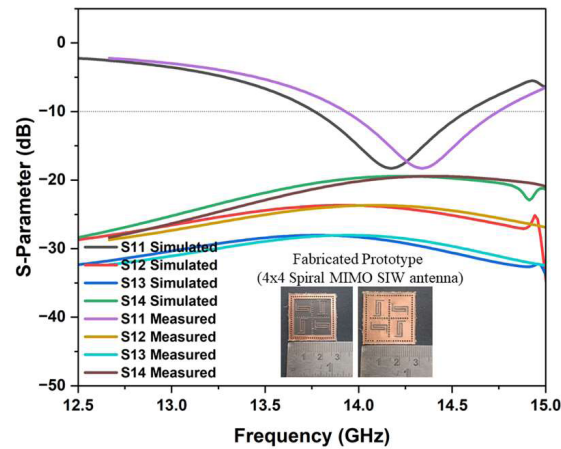


FIGURE 10. Measured and simulated S -parameter plots of proposed 4×4 spiral MIMO SIW antenna resonating at 14.17 GHz with bandwidth of 810 MHz.

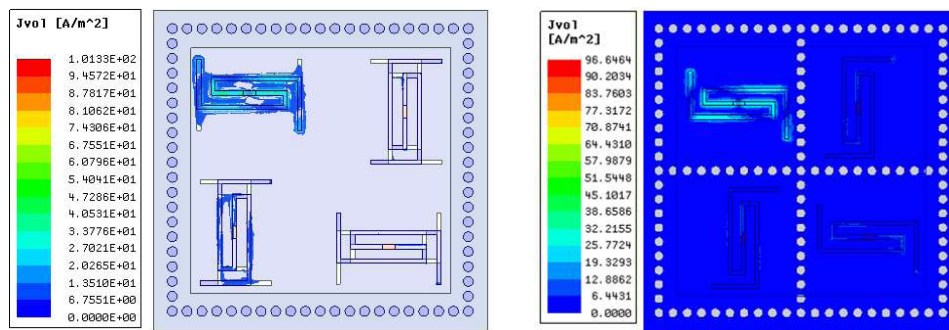


FIGURE 11. Surface current distribution of proposed 4×4 MIMO SIW antenna (when antenna 1 is excited without and with series of metal pin wall).

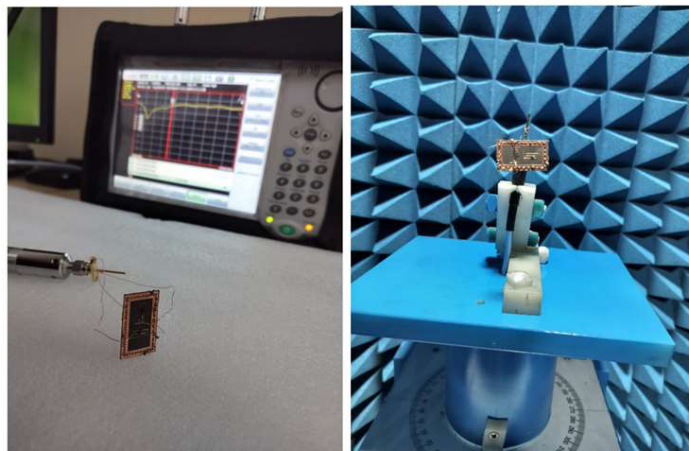


FIGURE 12. Measurement setup of CCBSSA MIMO with Vector Network Analyzer (VNA) and in Anechoic chamber.

antenna cell, hence avoiding any interference or leakage to the neighboring elements like shown in Fig. 11 (without metal pin wall).

The dimension of proposed 4×4 MIMO CCBSSA is $27.1 \times 27.1 \times 0.508 \text{ mm}^3$, making it highly compact and suitable for systems and applications requiring less component space.

Fig. 12 shows measurement setup of MIMO CCBSSA using Vector Network Analyzer (VNA up to 30 GHz) and Anechoic chamber (up to 40 GHz).

Figure 13 shows the measured and simulated radiation patterns in E -plane and H -plane of the proposed antenna along $+z$ and $-z$ axes with respect to antenna plane at 14.25 GHz.

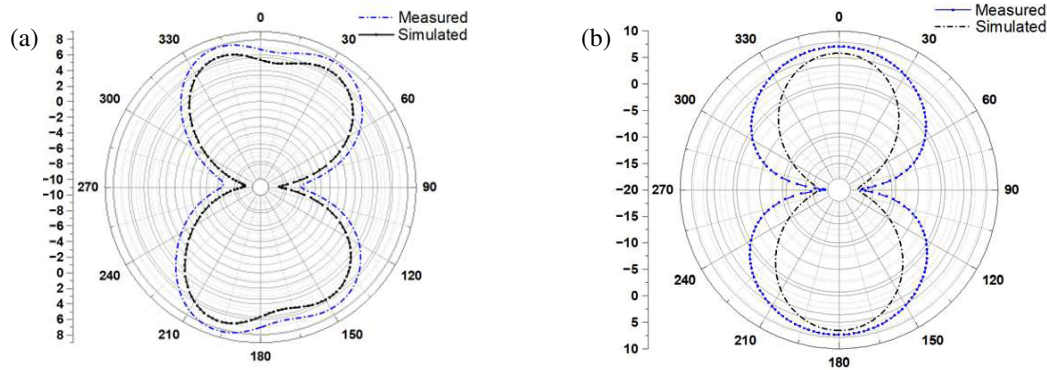


FIGURE 13. 2D radiation pattern of E -plane ($\phi = 0^\circ$) (a) and H -plane ($\phi = 90^\circ$) (b) in 4×4 MIMO SIW antenna at 14.25 GHz (measured).

TABLE 2. Comparison with existing literature.

Reference	Technology	Antenna Size (mm ²)	f_r (GHz)	FBW (%)	Return Loss (dB)	Gain (dBi)	ECC
[21] Sohi et al., 2020	Rectangular Spiral Microstrip MIMO	$34 \times 68.7 \times 3.25$	6.6	2.65	42.3	4.6	< 0.0009
[22] William et al., 2019	Traingular Spiral MIMO	$28 \times 20.5 \times 1.6$	3.79	-	24	3.7	0.08
[23] Alqadai et al., 2016	Microstrip wire spiral	$36 \times 43 \times 1.57$	5.15	0.04	18	3.45	-
[24] Saidi et al., 2023	Spiral microstrip button MIMO	13.6×20.1	5.5	0.04	23	7.2	< 0.05
[25] Padanathan et al., 2017	Tunable spiral MIMO microstrip	$120 \times 60 \times 1.6$	3.4	0.12	< -10	2.38	< 0.2
[26] Hashmi et al., 2022	spiral microstrip	$236 \times 272 \times 3$	0.433	47	< -10	7.4	-
Proposed Work	Spiral SIW MIMO	$27.1 \times 27.1 \times 0.508$	14.25	6.7	18.43	5.4	0.0001

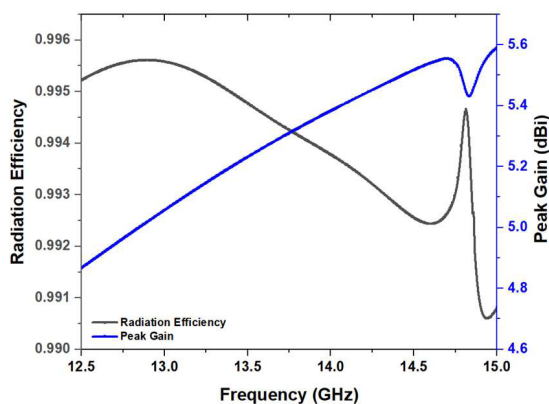


FIGURE 14. Radiation efficiency and peak gain in proposed 4×4 MIMO SIW antenna.

The beamwidth varies from -45° to $+45^\circ$ (i.e., beamwidth of 90°). The pattern diversity is achieved as antenna radiates in both the directions at $\theta = 0^\circ$ and $\theta = 90^\circ$. The radiation efficiency and gain plot is shown in Fig. 14. The proposed spiral MIMO SIW antenna radiates in elliptical polarization at the operating frequency band. It can be seen in Fig. 15 that the variation in current distribution at different phase excitations is shown. The plus shape isolation structure at the center of MIMO SIW antenna confines the field of each antenna by an electric field boundary, due to which the current in the dual spiral arms rotates from center port (+) to (-), towards one arm from 0° and 180° (i.e., Left hand polarization) and towards second arm from 180° to 360° (i.e., Right hand polarization). Thus, the proposed antenna shows both left-handed and right-handed elliptical polarization. The same can be verified from Fig. 16. The axial ratio value varies from 4.6 to 5.9 dB, and it

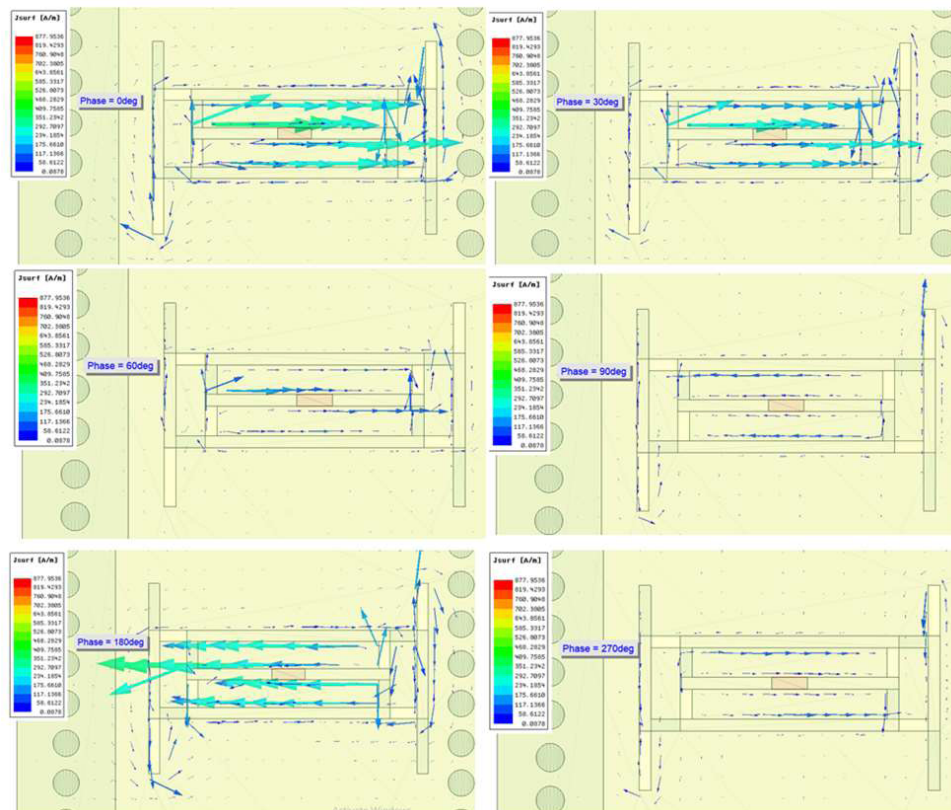


FIGURE 15. Surface current distributions at phase = 0 deg, 30 deg, 60 deg, 90 deg, 180 deg and 270 deg of proposed 4 × 4 spiral MIMO SIW antenna at 14.17 GHz (simulated).

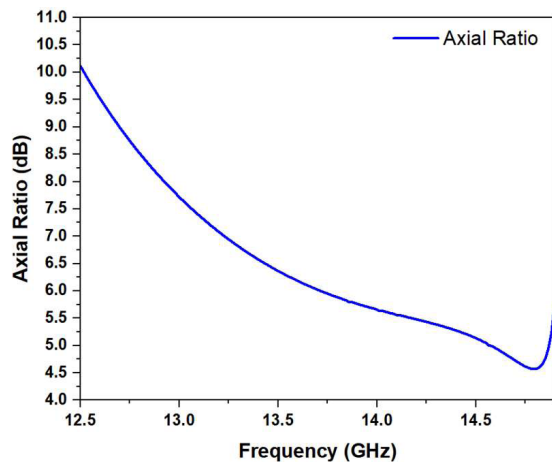


FIGURE 16. Simulated axial ratio plot of proposed MIMO SIW antenna at 14.17 GHz.

shows characteristics of elliptical polarization in the proposed 4 × 4 MIMO CCBSSA.

3.4. Diversity Performance Analysis of MIMO Antenna

Envelope correlation coefficient (ECC) and total active reflection coefficient (TARC) are essential parameters for evaluating the diversity performance of MIMO antennas. Low ECC values indicate that the antennas provide uncorrelated signal paths,

enhancing the diversity gain and overall system reliability. On the other hand, low TARC values reflect minimal active reflections and efficient antenna performance, contributing to higher efficiency and better signal quality. Together, these parameters help in optimizing the design and performance of MIMO systems for advanced wireless communication applications. ECC is a measure of how independently the multiple antennas in a MIMO system operate. The ECC between two antennas can be calculated using the *S*-parameters [27] from Equation (8).

$$ECC = \frac{|S_{11}^* S_{12} + S_{21}^* S_{22}|^2}{(1 - (|S_{11}|^2 + |S_{21}|^2))(1 - (|S_{12}|^2 + |S_{22}|^2))} \tag{8}$$

Ideally, ECC should be less than 0.05 for acceptable diversity performance, with values close to 0 indicating better performance. The proposed MIMO antenna achieves a good value of 0.0001 as shown in Fig. 17.

TARC is defined as the ratio of the square root of the sum of the reflected powers to the sum of the input powers for all ports in a MIMO system in Equations (9) and (10). A TARC value close to 0 means minimal active reflection, implying efficient transmission and minimal mutual coupling between antenna ports. In Fig. 17, it can be seen that the TARC value at 14.17 GHz is approximately -19 dB calculated from Equation (10) given in [28], showing efficient transmission of sig-

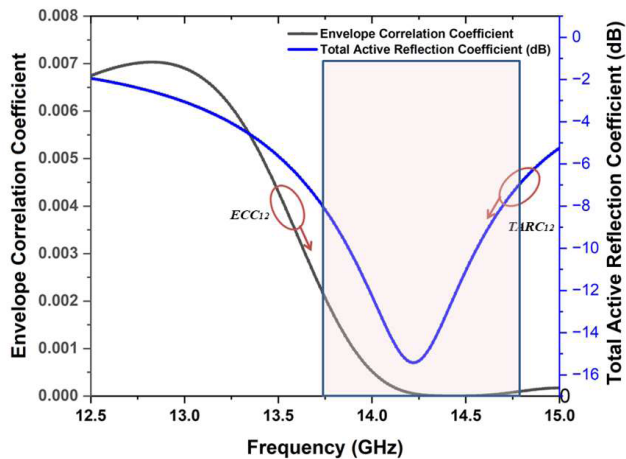


FIGURE 17. Envelope correlation coefficient (ECC_{12}) (in black) and total active reflection coefficient ($TARC_{12}$) (in blue) of proposed 4×4 MIMO SIW antenna design.

nals in MIMO antenna.

$$TARC = \frac{\sqrt{\sum_{i=1}^N |b_i|^2}}{\sqrt{\sum_{i=1}^N |a_i|^2}} \quad (9)$$

$$TARC = \frac{\sqrt{\left| \left(S_{11} + S_{12}^{e^{j\theta}} \right) \right|^2 + \left| \left(S_{21} + S_{22}^{e^{j\theta}} \right) \right|^2}}{\sqrt{2}} \quad (10)$$

Table 2 shows the comparison of proposed MIMO CCB-SSA antenna with existing literature in terms of size, resonant frequency, fractional bandwidth (FBW), return loss, gain, and ECC. The technology here is mainly microstrip, as very little work has been done in spiral SIW MIMO antenna. The spiral antennas designed in literature are designed at S and C bands only compared to proposed design working in Ku band.

4. CONCLUSION

The dual arm Archimedean spiral integrated with substrate integrated waveguide technology provides a miniaturized antenna design with minimum losses and high gain. The 4×4 MIMO antenna design achieves a high self-isolation using metal pins (in plus shape at center) of 19.6 dB at 14.17 GHz. The measured and simulated results almost match in S parameter plot and radiation pattern plot. As the gain increases from unit cell to 2×2 MIMO and 4×4 MIMO antennas, the bandwidth of antenna decreases from 970 MHz to 810 MHz (4×4 MIMO). Gain and bandwidth of an antenna have a trade-off. The diversity performance parameters like ECC and TARC show good isolation and minimum reflection in proposed CBSSA MIMO antenna, with values within acceptable limits. The structure with small size and high performance is suitable for applications in radio telescope, space communication, and Radar communication.

REFERENCES

- [1] Keith, M. J., S. Johnston, L. Levin, and M. Bailes, "17- and 24-GHz observations of southern pulsars," *Monthly Notices of the Royal Astronomical Society*, Vol. 416, No. 1, 346–354, 2011.
- [2] Ananthkrishnan, S., "The giant meterwave radio telescope," *Journal of Astrophysics and Astronomy*, Vol. 16, No. Sup, 427–435, 1995.
- [3] Sharma, P., R. N. Tiwari, P. Singh, P. Kumar, and B. K. Kanaujia, "MIMO antennas: Design approaches, techniques and applications," *Sensors*, Vol. 22, No. 20, 7813, 2022.
- [4] Desai, A., T. Upadhyaya, M. Palandoken, and C. Gocen, "Dual band transparent antenna for wireless MIMO system applications," *Microwave and Optical Technology Letters*, Vol. 61, No. 7, 1845–1856, 2019.
- [5] Desai, A., M. Palandoken, J. Kulkarni, G. Byun, and T. K. Nguyen, "Wideband flexible/transparent connected-ground MIMO antennas for sub-6 GHz 5G and WLAN applications," *IEEE Access*, Vol. 9, 147 003–147 015, 2021.
- [6] Wu, K. E., M. Bozzi, and N. J. G. Fonseca, "Substrate integrated transmission lines: Review and applications," *IEEE Journal of Microwaves*, Vol. 1, No. 1, 345–363, Jan. 2021.
- [7] Kumar, A., D. Chaturvedi, M. Saravanakumar, and S. Raghavan, "SIW cavity-backed self-triplexing antenna with T-shaped slot," in *2018 Asia-Pacific Microwave Conference (APMC)*, 1588–1590, Kyoto, Japan, Nov. 2018.
- [8] Kumar, A. and S. Srivastava, "A high-gain linear array of cross slots substrate integrated waveguide leaky-wave antenna with defective ground structure," *Microwave and Optical Technology Letters*, Vol. 64, No. 11, 2024–2029, 2022.
- [9] Chaturvedi, D., A. Kumar, A. A. Althwayb, and F. Ahmadfard, "SIW-backed multiplexing slot antenna for multiple wireless system integration," *Electronics Letters*, Vol. 59, No. 11, e12826, Jun. 2023.
- [10] Kumar, A. and S. I. Rosaline, "Hybrid half-mode SIW cavity-backed diplex antenna for on-body transceiver applications," *Applied Physics A*, Vol. 127, 1–7, 2021.
- [11] Tewari, N., N. Joshi, and S. Srivastava, "A circularly polarized cylindrical cavity backed substrate integrated waveguide antenna for millimeter wave applications," in *2022 IEEE Microwaves, Antennas, and Propagation Conference (MAPCON)*, 1562–1567, Bangalore, India, Dec. 2022.
- [12] Tewari, N. and N. Joshi, "A circularly polarized cross slot cavity backed substrate integrated waveguide antenna for 60 GHz applications," in *2022 8th International Conference on Signal Processing and Communication (ICSC)*, 1–5, Noida, India, Dec. 2022.
- [13] Spurek, J. and Z. Raida, "SIW-based circularly polarized antenna array for 60 GHz 5G band: Feasibility study," *Sensors*, Vol. 22, No. 8, 2945, 2022.
- [14] Tewari, N., N. Joshi, and S. Srivastava, "A novel reconfigurable H-plane Horn leaky wave Substrate Integrated Waveguide MIMO antenna for K band," *AEU — International Journal of Electronics and Communications*, Vol. 170, 154832, 2023.
- [15] Tewari, N., N. Joshi, and S. Srivastava, "A miniaturized aperture-coupled 4×4 MIMO array SIW antenna at K band," *Microwave and Optical Technology Letters*, Vol. 66, No. 1, e33952, 2024.
- [16] Balanis, C. A., *Antenna Theory: Analysis and Design*, John Wiley & Sons, 2015.
- [17] Pandey, A. K., N. K. Sahu, R. K. Gangwar, and R. K. Chaudhary, "A SIW-cavity-backed wideband circularly polarized antenna using modified split-ring slot as a radiator for mm-Wave

- IoT applications,” *IEEE Internet of Things Journal*, Vol. 11, No. 7, 11 793–11 799, Apr. 2024.
- [18] Eid, A. M., A. A. Salama, and H. M. Elkamchouchi, “A novel wide bandwidth antenna array using slotted spiral SIW for satellite communications,” in *2020 IEEE 10th International Conference on Consumer Electronics (ICCE-Berlin)*, 1–5, Berlin, Germany, 2020.
- [19] Xu, F. and K. Wu, “Guided-wave and leakage characteristics of substrate integrated waveguide,” *IEEE Transactions on Microwave Theory and Techniques*, Vol. 53, No. 1, 66–73, 2005.
- [20] Kaiser, J., “The Archimedean two-wire spiral antenna,” *IRE Transactions on Antennas and Propagation*, Vol. 8, No. 3, 312–323, May 1960.
- [21] Sohi, A. K. and A. Kaur, “UWB aperture coupled circular fractal MIMO antenna with a complementary rectangular spiral defected ground structure (DGS) for 4G/WLAN/radar/satellite/international space station (ISS) communication systems,” *Journal of Electromagnetic Waves and Applications*, Vol. 34, No. 17, 2317–2338, 2020.
- [22] William, J., P. Bhat, M. Gaonkar, S. Gaonkar, S. Khandekar, and R. Patil, “Design and analysis of MIMO spiral antenna for GPS, WLAN and UAV applications,” *European Journal of Engineering and Technology Research*, Vol. 4, No. 8, 130–134, 2019.
- [23] Alqadami, A. S. M., M. F. Jamlos, P. J. Soh, S. K. A. Rahim, and A. Narbudowicz, “Left-handed compact MIMO antenna array based on wire spiral resonator for 5-GHz wireless applications,” *Applied Physics A*, Vol. 123, 64, 2017.
- [24] Saeidi, T., A. J. A. Al-Gburi, and S. Karamzadeh, “A miniaturized full-ground dual-band MIMO spiral button wearable antenna for 5G and sub-6 GHz communications,” *Sensors*, Vol. 23, No. 4, 1997, 2023.
- [25] Padmanathan, S., A. A. Al-Hadi, P. J. Soh, and M. F. Jamlos, “A compact two-port tunable dual-band spiral antenna for MIMO terminals,” in *2017 International Symposium on Antennas and Propagation (ISAP)*, 1–2, Phuket, Thailand, 2017.
- [26] Hashmi, M. A. R. and P. V. Brennan, “A low profile wideband RHCP printed Archimedean spiral antenna for glacial telemetry applications,” in *2022 Asia-Pacific Microwave Conference (APMC)*, 632–634, Yokohama, Japan, Nov. 2022.
- [27] Sharawi, M. S., “Printed multi-band MIMO antenna systems and their performance metrics [wireless corner],” *IEEE Antennas and Propagation Magazine*, Vol. 55, No. 5, 218–232, 2013.
- [28] Pei, T., L. Zhu, J. Wang, and W. Wu, “A low-profile decoupling structure for mutual coupling suppression in MIMO patch antenna,” *IEEE Transactions on Antennas and Propagation*, Vol. 69, No. 10, 6145–6153, 2021.